Journal of Magnetics 9(1), 17-22 (2004)

Magnetic Tunnel Junctions with AlN and AlO Barriers

Tae Sick Yoon[1,2], Satoru Yoshimura[2], Masakiyo Tsunoda[2], Migaku Takahashi[2], Bum Chan Park[1], Young Woo Lee[1], Ying Li[3] and Chong Oh Kim[1,*]

[1]*Research Center for Advanced Magnetic Materials, Chungnam National University, Daejeon 305-764, Korea*
[2]*Department of Electronic Engineering, Tohoku University, Sendai 980-8579, Japan*
[3]*Institute of Materials, School of Materials Science and Engineering, Shanghai University, P.R. China*

(Received 7 January 2004)

We studied the magnetotransport properties of tunnel junctions with AlO and AlN barriers fabricated using microwave-excited plasma. The plasma nitridation process provided wider controllability than the plasma oxidization for the formation of MTJs with ultra-thin insulating layer, because of the slow nitriding rate of metal Al layers, comparing with the oxidizing rate of them. High tunnel magnetoresistance (TMR) ratios of 49 and 44% with respective resistance-area product ($R \times A$) of 3×10^4 and 6×10^3 Ωμm² were obtained in the Co-Fe/Al-N/Co-Fe MTJs. We conclude that AlN is a hopeful barrier material to realize MTJs with high TMR ratio and low $R \times A$ for high performance MRAM cells. In addition, in order to clarify the annealing temperature dependence of TMR, the local transport properties were measured for Ta 50 Å/Cu 200 Å/Ta 50 Å/$Ni_{76}Fe_{24}$ 20 Å/Cu 50 Å/$Mn_{75}Ir_{25}$ 100 Å/$Co_{71}Fe_{29}$ 40 Å/Al-O junction with $d_{Al} = 8$ Å and $P_{O2} \times t_{OX} = 8.4 \times 10^4$ L at various temperatures. The current histogram statistically calculated from the electrical current image was well in accord with the fitting result considering the Gaussian distribution and Fowler-Nordheim equation. After annealing at 340 °C, where the TMR ratio of the corresponding MTJ had the maximum value of 44%, the average barrier height increased to 1.12 eV and its standard deviation decreased to 0.1 eV. The increase of TMR ratio after annealing could be well explained by the enhancement of the average barrier height and the reduction of its fluctuation.

Key words : Tunnel junctions, AlN barrier, AlO barrier, Microwave-excited plasma, Nitridation process, Local transport properties, Fowler-Nordheim equation

1. Introduction

Magnetic tunnel junctions (MTJs) consisting of two ferromagnetic layers separated by a thin insulating layer have attracted much attention due to their potential application for nonvolatile magnetic random access memories (MRAMs) [1, 2]. High TMR ratio and low resistance-area product ($R \times A$) of MTJs is important to realize MRAMs with low error rate and fast operation speed [3]. In order to achieve these properties, the formation process of very thin insulating layer should be precisely controlled. Although the plasma oxidization of metal Al layer is generally accepted to be a suitable method to obtain high TMR ratio in MTJs, its high-reactivity makes it difficult to oxidize ultra-thin Al layer precisely down to the interface of the lower ferromagnetic electrode. The nitridation process of metal Al films is expected to progress mildly than the oxidization process of metal Al films, from the aspects of affinity of reactive gases for metals and the lower diffusion coefficient of nitrogen in the insulator than that of oxygen [4]. However, the highest TMR ratio, which has been reported for the MTJs with AlN layer, is only 33% [5] and smaller than that of the MTJs with AlO barrier. This seems to be an obstacle to utilize the AlN layer as a tunnel barrier of MTJs.

In the present study, we investigate the formation process of AlN layer in MTJs fabricated by microwave-excited plasma nitridation method through the magnetotransport properties of MTJs, comparing with the oxidation process. Since the change of inert gas mixed into oxygen for the plasma oxidization process is effective to improve the magnetotransport properties of MTJs with AlO [6], we also discuss the effect of inert gas mixed into nitrogen on the magnetotransport properties of MTJs with AlN. Furthermore, we report the local transport properties on

*Corresponding author: Tel: +82-42-821-6234, e-mail: magkim@cnu.ac.kr

© 2004 Journal of Magnetics

ferromagnetic tunnel junction measured using conducting atomic force microscope (C-AFM). The significance of this technique is that it can simultaneously record the usual topographical information and map, at the nanometric scale, local current transmitted through a tunnel barrier consisting of an insulating layer, when constant bias voltage is applied between the tip and the ferromagnetic film, which lies below the insulating barrier [7, 8]. Thus, the information of local barrier characteristic, which may arise from defects providing localized electron states, pinholes in the insulating films and fluctuations in barrier height, can be observed [9]. The system studied here is based on insulating layer, used as a tunnel barrier in our tunnel junctions.

2. Experimental Procedure

Tunnel junctions with the structure of Ta 50 Å / Cu 200 Å / Ta 50 Å / $Ni_{76}Fe_{24}$ 20 Å / Cu 50 Å / $Mn_{75}Ir_{25}$ 100 Å / $Co_{71}Fe_{29}$ 40 Å / Al-N or Al-O/$Co_{71}Fe_{29}$ 40 Å / $Ni_{76}Fe_{24}$ 200 Å / Ta 50 Å were prepared on thermally oxidized Si wafers. All the metallic films were deposited by dc magnetron sputtering method. The barrier formation was performed by depositing a metal Al film with thickness, d_{Al} = 8, 10, 15 Å, and subsequently nitridizing or oxidizing it in the chamber with radial line slot antenna (RLSA) for 2.45 GHz microwave [6, 10]. The mixing concentration of nitrogen and oxygen into inert gas were 5% and 0.5~3%, respectively. The nitridation and oxidation time were 10~150 s and 1~40 s, respectively. The applied microwave power density was 1.1 W/cm^2. A photolithography process and ion milling were used to pattern the tunnel junctions in normal area of 25~2500 μm^2. The TMR measurements were performed with a four-point probe method at a bias voltage of 5 mV. The scaling of the resistance inversely with the area of the junction and the constant TMR regardless of the size of the junction excluded the possibility of geometrical enhancement of the TMR. The thermal treatment consisted of consecutive 60-min vacuum annealing at each temperature, followed by furnace field cooling (1 kOe).

In order to investigate the local transport properties, tunnel junction of Ta 50 Å / Cu 200 Å / Ta 50 Å / $Ni_{76}Fe_{24}$ 20 Å / Cu 50 Å / $Mn_{75}Ir_{25}$ 100 Å / $Co_{71}Fe_{29}$ 40 Å / Al-O was fabricated. The thickness of metal Al layer, oxidation time, and concentration of oxygen mixing into inert gas were 8 Å, 7 s, and 3%, respectively. The MTJ oxidized in the oxidization chamber was transferred into the AFM chamber, and all the measurements were performed at room temperature under the pressure below 5×10^{-6} Torr after annealing the junction at a temperature between 300 and 360 °C. After fixing the cantilever at the one site of barrier layer, the local *I-V* curves were measured. The local *I-V* curves were measured at about 10 points of the current images, and then the average barrier height ϕ_{ave} and width *D* of the junction were estimated using Simmons' formula, where data within ±1.5 V were used for fitting and contact area of 1 nm^2 was assumed.

3. Results and Discussion

Fig. 1 shows the resistance-area product ($R \times A$) of as-prepared MTJs with d_{Al} = 8, 10, 15 Å, fabricated with the various condition of nitridation or oxidation using Ar + N_2, Kr + N_2, Ar + O_2, and Kr + O_2 plasma. The horizontal axis corresponds to the amount of plasma exposure, represented by the product of the partial pressure of nitrogen / oxygen and the exposing time for nitridation / oxidation plasma, where 1 L (Langmuir) is defined as 1×10^{-6} Torr·sec. The needed amount of nitrogen exposure is 1~2 orders larger than that of oxygen exposure during the plasma nitridation / oxidation process, to obtain a same $R \times A$ value. It indicates that the nitriding rate of metal Al film is quite slow in comparison with the oxidizing rate of metal Al film, as expected. When we attend to the effect of inert gas, the $R \times A$ of the MTJs with Al(15 Å)-O (inverse triangle) fabricated with Kr + O_2 plasma is obviously higher than that of the MTJs fabricated with Ar + O_2 plasma under the same amount of plasma exposure. On the other hand, the $R \times A$ of MTJs with Al-N does not strongly depend on the sort of inert gas and is slightly higher for the Kr + N_2 case than for the Ar + N_2 case. This is due to the difference of inert gas effect on

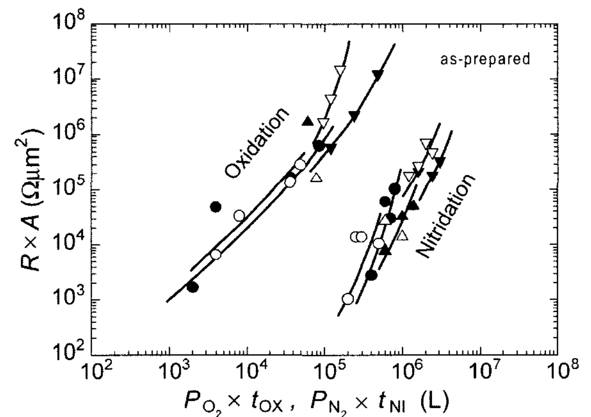

Fig. 1. Resistance-area product of as-prepared MTJs with the Al layer thickness of 8 Å (circle), 10 Å (triangle), 15 Å (inverse triangle), fabricated with various conditions of nitridation or oxidation. The horizontal axis corresponds to the amount of plasma exposure. Ar (closed symbols) and Kr (open symbols) are used as the mixed inert gases.

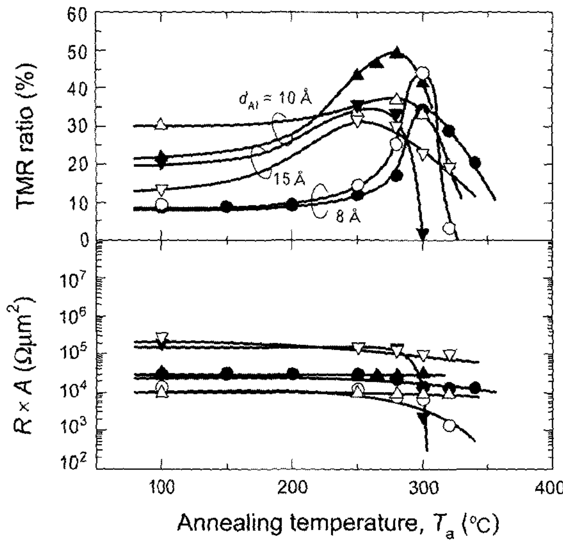

Fig. 2. Annealing temperature dependence of TMR ratio and resistance-area product for the MTJs with various metal Al layer thickness of 8 Å (circle), 10 Å (triangle), 15 Å (inverse triangle), fabricated with $Ar+N_2$ (closed symbols) and $Kr+N_2$ (open symbols) plasma.

excitation of reactive species in plasma between the oxidization process and the nitridation process. We otherwise confirmed through the optical emission spectroscopy that the reactive species in nitridation plasma does not change with changing the inert gas between Ar and Kr, in contrast with the fact that very active O^1D radicals are excited more effectively in the $Kr + O_2$ plasma than in the $Ar + O_2$ plasma [11].

Fig. 2 shows the changes of the TMR ratio and the $R \times A$ of the MTJs with various Al layer thickness fabricated using $Ar + N_2$ or $Kr + N_2$ plasma, as a function of annealing temperature. The nitridation condition, in other words, the amount of nitridation plasma exposure, is optimized to maximize the achievable TMR ratio of MTJs during thermal annealing, for respective metal Al layer thickness. The data plotted at 100 °C correspond to those for the as-prepared MTJs. Regardless of the Al layer thickness, TMR ratio increases with increasing T_a and takes maximum at a certain temperature, and then decreases. When the metal Al thickness is varied from 15 to 8 Å, the annealing temperature where the TMR ratio reaches its maximum shifts from 250 to 300 °C. High TMR ratio of 49% and 44% are obtained at $T_a = 280$ and 300 °C for MTJs with $d_{Al} = 10$ and 8 Å, respectively. These TMR ratios are much larger than the values that have ever been reported for the CoFe/Al-N/CoFe tunnel junctions and are comparable to the CoFe/Al-O/CoFe junctions. Taking into account the $R \times A$ value of 3×10^4 $\Omega\mu m^2$ for TMR ratio of 49% and 6×10^3 $\Omega\mu m^2$ for TMR ratio of 44%, one says that these MTJs satisfy the specification for 1 Gbit MRAM cells [12].

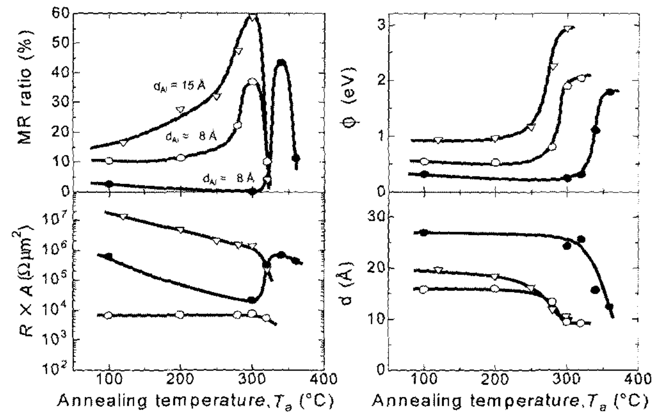

Fig. 3. Annealing temperature dependence of TMR ratio, resistance-area product, barrier height, and barrier width for the MTJs with various Al layer thickness and oxidation condition. Plasma oxidization condition is $P_{O2} \times t_{OX} = 4.0 \times 10^3$ L (○), 8.4×10^4 L (●), and 1.6×10^5 L (▽), respectively.

The changes of the TMR ratio, $R \times A$, and barrier characteristics of the MTJs with Al-O barrier against T_a are shown in Fig. 3. The d_{Al} are 8 and 15 Å. The amount of oxygen exposure are 4.0×10^3 L (○ , $P_{O2} = 0.5\%$, t_{OX} = 2 s, $Kr+O_2$ plasma) or 8.4×10^4 L (● , $P_{O2} = 3\%$, t_{OX} = 7 s, $Ar+O_2$ plasma) for the d_{Al} = 8 Å case, and 1.6×10^5 L (▽ , $P_{O2} = 3\%$, t_{OX} = 13 s, $Kr+O_2$ plasma) for the d_{Al} = 15 Å case, respectively. For the case of d_{Al} = 8 Å with $P_{O2} \times t_{OX} = 4.0 \times 10^3$ L and d_{Al} = 15 Å with $P_{O2} \times t_{OX} = 1.6 \times 10^5$ L, the TMR ratio takes maximum at T_a = 300 °C, regardless of the Al layer thickness, and $R \times A$ slightly decreases with increasing T_a, similar to the MTJ with Al-N layer shown in Fig. 2. On the other hand, in the case of d_{Al} = 8 Å with $P_{O2} \times t_{OX} = 8.4 \times 10^4$ L, the high TMR ratio of 44% are unexpectedly obtained at very high annealing temperature of 340 °C, whereas the TMR ratio is very low at T_a less than 300 °C. At the same time, $R \times A$ decreases for annealing up to 300 °C, and then rapidly increases up about one order over 300 °C. These behaviors are generally observed in the so-called 'over oxidized' MTJs [13], and are characterized by the sudden increase of TMR accompanied with the significant increase of $R \times A$. Taking into account this, we can say that MTJs with Al-N layer shown in Fig. 2 and MTJs with Al-O layer, indicated by open symbols in Fig. 3, are not 'over nitrided/oxidized' junctions and might be optimized to nitride/oxidize the metal Al layer precisely down to the interface of the lower ferromagnetic electrode for respective metal Al layer thickness.

Fig. 4 shows the current images for the junction with AlO barrier annealed at various temperatures. The scann-

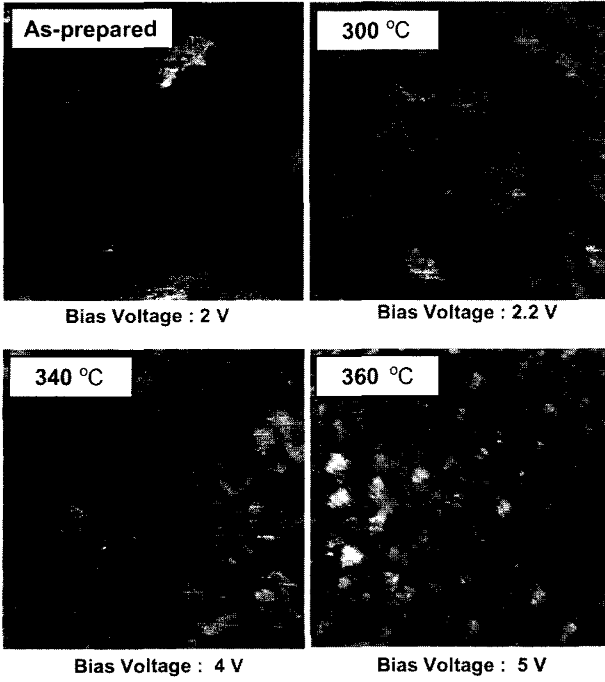

Fig. 4. Current images of Ta 50 Å / Cu 200 Å / Ta 50 Å / $Ni_{76}Fe_{24}$ 20 Å / Cu 50 Å / $Mn_{75}Ir_{25}$ 100 Å / $Co_{71}Fe_{29}$ 40 Å / Al-O junction with d_{Al} = 8 Å and $P_{O2} \times t_{OX} = 8.4 \times 10^4$ L as a function of annealing temperature. The scanning area is 300 × 300 nm^2.

ing area is 300 × 300 nm^2. The values of the external bias voltages are also shown in the figure. The bright region indicates the local transport sites with high conductance. The contrast of current image for the as-prepared junction is very high, namely, junction has a large current distribution and relatively high currents flow through different localized sites [8, 14]. However, the contrast of current image for the junction after annealing at 340 °C is very low. After further annealing at 360 °C, the contrast in the current image becomes high again. In order to clarify the relationship between the contrast and TMR, the following calculation was carried out. From the *I-V* curves of some local points of the junction, the contrast of the electrical current image was known to offer information about the distribution of local barrier height [7, 8, 14]. The variation of barrier height was presumed to submit the Gaussian distribution with the average barrier height ϕ_{ave} and the standard deviation σ_ϕ taken as follows:

$$P(\phi) = \frac{1}{\sqrt{2\pi}\sigma_\phi}\exp\left(\frac{-(\phi(I) - \phi_{ave})^2}{2\sigma_\phi^2}\right). \tag{1}$$

Here, ϕ_{ave} is the mean of barrier height obtained from local *I-V* curves. Because the Simmons' formula is appli-

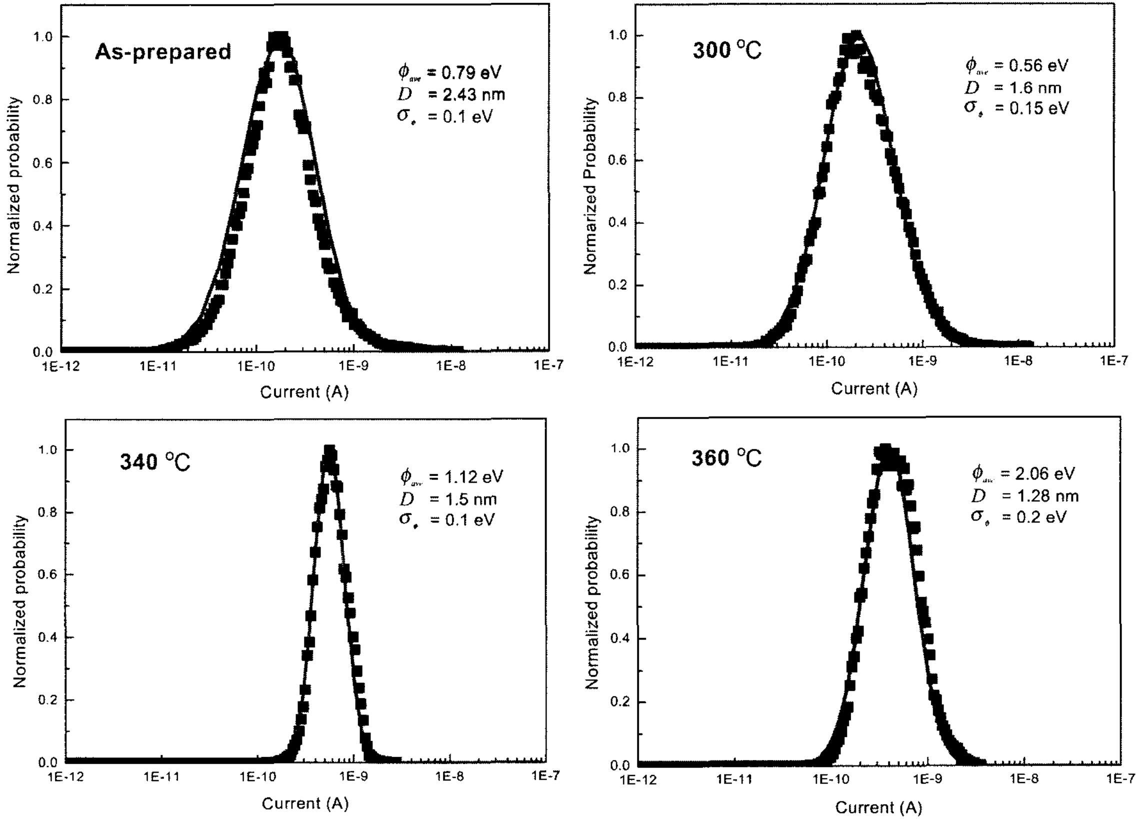

Fig. 5. Current distribution statistically calculated from the electrical current images is indicated by squares. Solid lines are the best-fitted results considering the gaussian distribution and F-N equation.

cable only for bias voltage smaller than the barrier height [15], the current through the barrier could be given by Fowler-Nordheim (F-N) equation as follows [7]:

$$I = A\frac{V^2}{\phi D^2}\exp\left(-B\frac{D\phi^{3/2}}{V}\right), \tag{2}$$

where, I and V indicate the current and the bias voltage, respectively. A, as a fitting parameter, is the effective emission area calculated from the center of current histogram [8, 14]. The field enhancement factor B arising from the nonplanar geometry of the tip is defined as 0.5 [7, 14]. D is the values of the average barrier width obtained from I-V curves. The histogram of current density with parameters of the average barrier height ϕ_{ave} and its standard deviation σ_ϕ was calculated by the equation (1) and (2). And then it was fitted to current distribution calculated from the electrical image.

Fig. 5 shows the best-fitted results by the above-mentioned method. The square shows the current distribution statistically calculated from the electrical current images and the solid lines are the fitting results considering the Gaussian distribution and F-N equation. The ϕ_{ave} and D, which is from the local I-V characteristics, and σ_ϕ from fitting are also shown in the figure. The fitting results as a function of annealing temperature correspond well to the current histogram obtained from the electrical images. For the case of junction with small contrast after annealing at 340 °C, ϕ_{ave} increased to 1.12 eV and σ_ϕ decreased to 0.1 eV. After further annealing at 360 °C, the standard deviation increased to 0.2 eV. As a result, the oxidization process can be explained as follows: in the as-prepared junction, it is considered that oxygen moves down to the surface of lower ferromagnetic electrode through the grain boundaries rather than the inner grain of metal Al layer, since the diffusing mobility of oxygen is generally larger at the grain boundaries than the inner grain. After annealing at 340 °C, oxygen existing on the underlaid ferromagnetic electrode surface will homogeneously diffuse into the grains of Al-oxide layer, where the barrier layer has so stable composition that the homogenous insulating layer with the high barrier height and the low σ_ϕ is formed. For annealing at the higher temperature than 360 °C, the local generation of a low barrier height due to interface mixing between insulator and electrode, and/or the growth of grains at the bottom of the electrode will be happened. That is, the insulator would be separated into two regions, high barrier height regions with sufficient oxygen and low barrier height regions with less oxygen, which cause the increase of standard deviation σ_ϕ, resulting in the decrease of TMR ratio. Consequently, the high TMR ratio of 44% at very high annealing temperature of 340 °C can be well described as the increase of ϕ_{ave} and the decrease of $\sigma_\phi \cdot \phi_{ave}$ and D from local I-V curves are well in agreement with the barrier height (ϕ) and width (d) for the junction shown in Fig. 3.

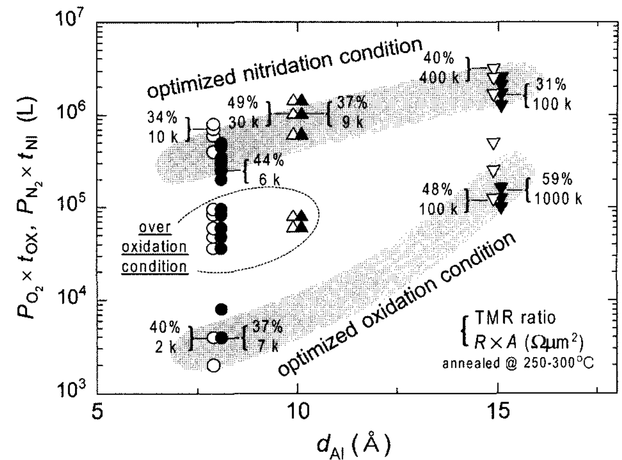

Fig. 6. The amount of nitrogen or oxygen exposure during the plasma process of metal Al film of MTJs as a function of d_{Al}. Ar (closed symbols) and Kr (open symbols) are used as the mixed inert gases.

Fig. 6 shows the result of nitrogen or oxygen exposure amount re-plotted against d_{Al} for the MTJs represented in Fig. 1. The TMR ratio and $R \times A$ value obtained after annealing the junction at a temperature between 250 and 300 °C are attached for several MTJs. The shaded areas indicate the optimized nitridation/oxidization condition to obtain high TMR ratio for respective d_{Al}. When d_{Al} is varied from 15 to 8 Å, the required amounts of oxygen exposure decrease rapidly, but that of nitrogen exposure decrease gradually. It means that the optimized nitridation condition is less sensitive to the metal Al layer thickness than that of oxidization. That is, the plasma nitridation process provides wider controllability than the oxidization process for the formation of MTJs with ultra-thin barrier.

4. Conclusion

We succeeded to induce large TMR ratio of 49% in MTJs with AlN barrier, which is comparable to the MTJs with AlO barrier, and found that the nitridation process of ultra-thin Al layer has wider controllability than the oxidization process. Also, we investigated correlation between the local transport properties of the tunnel barrier with the quantities obtained from measuring patterned the tunnel junctions, so it was clarified that enhancement of ϕ_{ave} and the reduction of its fluctuation must be precisely controlled to achieve a high TMR ratio.

Acknowledgements

This work was supported by the Korean Science and Engineering Foundation through the Research Center for Advanced Magnetic Materials at Chungnam National University.

References

[1] S. S. S. Parkin, et al., J. Appl. Phys. **85**, 5828 (1999).
[2] L. Pust, L. E. Wenger, R. A. Lukaszew, Y. Sheng, D. Litvinov, Y. Wang, C. Uher, and R. Clarke, J. Appl. Phys. **85**, 5765 (1999).
[3] K. Inomata, J. Magn. Soc. of Japan **23**, 1826 (1999).
[4] W. D. Kingery, Physics of Ceramic Materials (1980).
[5] Jianguo Wang, S. Cardoso, P. P. Freitas, P. Wei, N. P. Barradas, and J. C. Soares, J. Appl. Phys. **89**, 6868 (2001).
[6] K. Nishikawa, S. Ogata, T. Syoyama, W. S. Cho, T. S. Yoon, M. Tsunoda, and M. Takahashi, Journal of Magnetics **7**, 63 (2002).
[7] Y. Ando, H. Kameda, H. Kubota, and T. Miyazaki, J. Appl. Phys. **87**, 5206 (2000).
[8] T. S. Yoon, M. Tsunoda, M. Takahashi, C. G. Kim, and C. O. Kim, J. Kor. Magn. Soc. **13**, 47 (2003).
[9] T. Dimopoulos, V. D. Costa, C. Tiusan, K. Ounadjela, and H. Van, J. Appl. Phys. **89**, 7371 (2001).
[10] M. Tsunoda, K. Nishigawa, S. Ogata, and M. Takahashi, Appl. Phys. Lett. **80**, 3135 (2002).
[11] S. Yoshimura, M. Tsunoda, S. Ogata, and M. Takahashi, to be published in J. Magn. Soc. Jpn. (2003).
[12] S. Tehrani, et al., Proceedings of the IEEE **91**, 703 (2003).
[13] S. Iura, H. Kubota, Y. Ando, and T. Miyazaki, J. Magn. Soc. Jpn. **27**, 303 (2003).
[14] T. S. Yoon, M. Tsunoda, M. Takahashi, C. G. Kim, and C. O. Kim, Kor. J. Mater. Resea. **13**, 233 (2003).
[15] J. G. Simmons, J. Appl. Phys. **34**, 1793 (1963).